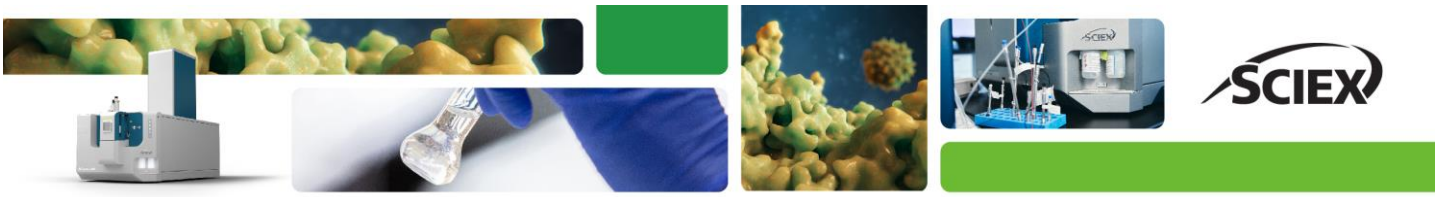

Quantification and impurity analysis of ALC-0315 from LNPs in plasma using the ZenoTOF 7600 system

Daniel Zimmer[1], Matthew D Stone[2], Robert Proos[2], Santosh Kupil Kumar Gorti[2], Mays Al-Dulaymi[3], Paul RS Baker[2], and Christina M Bailey-Hytholt[1]

[1]Dept of Chemical Engineering, Worcester Polytechnic Institute, Worcester, MA; [2]SCIEX, USA, [3]SCIEX, Canada

In this technical note, the ZenoTOF 7600 system was used to sensitively quantitate the ionizable lipid ALC-0315 and structurally elucidate its related impurities from lipid nanoparticles (LNPs) in plasma. Due to its inherent sensitivity, a triple quadrupole mass spectrometer (TQMS) is typically used for targeted bioanalytical quantitation. However, collision-induced dissociation (CID)-based lipid fragmentation is insufficient for their complete structural characterization. The ZenoTOF 7600 system is capable of sensitive, targeted quantitation and can utilize a complimentary fragmentation mode (electron-activated dissociation; EAD), which is effective for confident metabolic identification (MetID) (1-3) and the structural elucidation of lipids (4-9), thereby adding unique value for analytical versatility.

To demonstrate the quantitative performance of the ZenoTOF 7600 system for bioanalysis of ALC-0315, quantitation curves with lower limits of quantitation (LLOQs) were determined using either a precursor-to-fragment or precursor-to-precursor high-resolution MRM (MRM^{HR}), and the amount of ALC-0315 from formulated LNPs diluted into plasma was then estimated. Impurities related to ALC-0315 at relative abundances as low as 0.02% were observed from the LNPs and some of the structures of these impurities were elucidated using EAD (**Figure 1**).

Key features of ionizable lipid analysis on the ZenoTOF 7600 system

- Through MRM^{HR} acquisition, the ZenoTOF 7600 system can detect and quantitate ionizable lipids at sub ng/mL levels from formulated LNPs
- The simultaneous acquisition of full product ion spectra during quantitative analysis allows verification of other components within LNPs, such as the PEGylated lipid and structures related to the ionizable lipid
- EAD coupled with the Zeno trap allows for confident structural elucidation of low-level impurities associated with the ionizable lipid, demonstrating its usefulness in supporting MetID studies

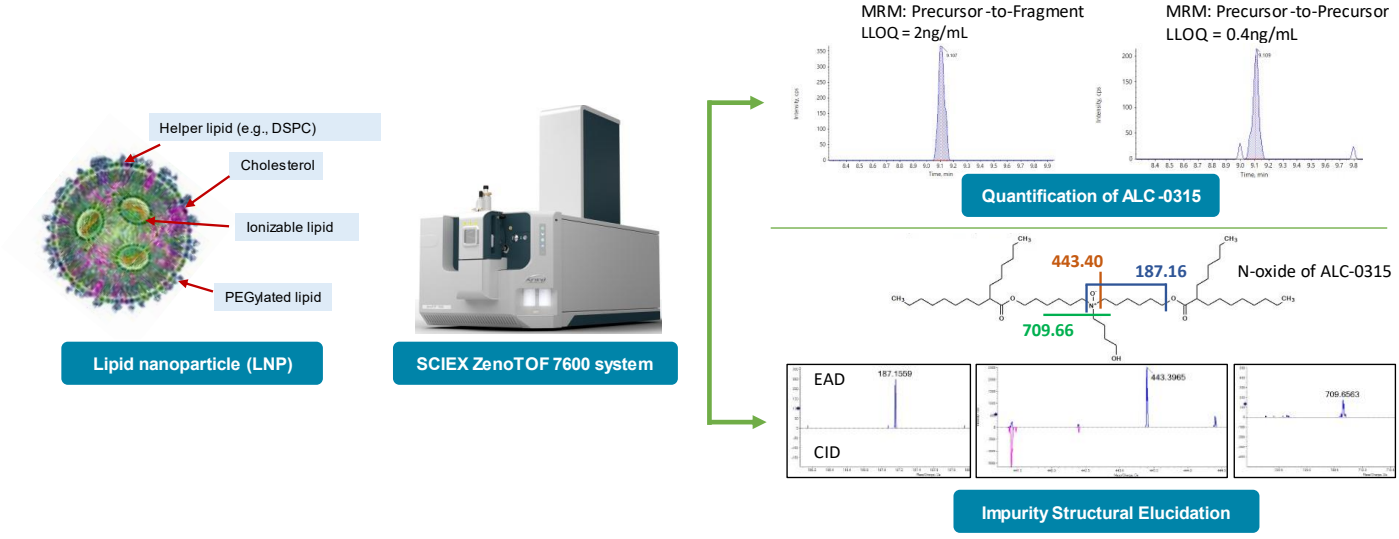

Figure 1. Versatility of the ZenoTOF 7600 system to support quantitation and characterization workflows for analysis of the ionizable lipid ALC-0315 from LNPs. Upper right panel: Representative peak areas of the LLOQ of ALC-0315 diluted into plasma from precursor-to-fragment MRM^{HR} (m/z 766.72 to 510.49) or precursor-to-precursor MRM^{HR} (766.72 to 510.49). The precursor-to-precursor MRM provided the greatest sensitivity. Bottom right panel: Identification of the N-oxide impurity of ALC-0315 from LNPs diluted in plasma. Three distinct fragment ions from EAD of m/z 187.16, 443.40, and 709.66 not observed by CID were used to isolate the site of oxygen incorporation to the tertiary amine to confirm N-oxidation.

Introduction

LNPs have emerged as safe and effective delivery vehicles for oligonucleotide-based therapeutics such as the siRNA-based Onpattro as well as messenger RNA (mRNA)-based vaccines such as Spikevax and Comirnaty (10). This has spawned investment into new precision genetic medicines by designing novel lipids to fine-tune properties like targeted delivery, biodegradation, and endosomal escape. LNPs typically comprise ionizable lipids, helper lipids such as distearoylphosphatidylcholine (DSPC), cholesterol, and PEGylated lipids (**Figure 1**). For example, the LNPs used in the Pfizer/BioNTech COVID-19 vaccine contained ALC-0315, DSPC, cholesterol, and PEG2000 conjugated lipid.

With the administration of novel exogenous materials, like the ionizable lipids used in LNPs, it is necessary to track their biodistribution and metabolism products to assess their safety and efficacy profiles. TQMSs are used for quantification studies to support bioanalytical assays using an MRM approach. However, some lipids may not fragment well by traditional CID fragmentation techniques nor produce diagnostic product ions to distinguish them from other interfering ions within biological matrices. In addition, it can be challenging to identify the structures of compounds formed from degradation or metabolism using a CID-based fragmentation alone. It has been shown that EAD-based fragmentation can produce information-rich spectra that can confidently elucidate structures of ionizable lipids and pinpoint sites of modifications within their related impurity structures (11-13).

In this study, we assessed the ability of the ZenoTOF 7600 system to quantify ALC-0315 in plasma. This instrument includes a Zeno trap device that enhances MS/MS sensitivity to drive quantitative sensitivity. In addition, the instrument can provide complementary fragmentation via EAD to aid in structural characterization. Both aspects of the instrument were used to quantify and provide in-depth characterization of impurities related to ALC-0315 to demonstrate its utility in supporting LNP metabolism studies.

Materials and methods

Materials: ALC-0315 was purchased from Broadpharm (Cat #BP-25498) or Caymen Chemical (Cat #34337). DSPC (Cat #850365), cholesterol (CAT # 700100), and 1,2-dimyristoyl-sn-glycero-3-phosphoethanolamine-N-[methoxy(polyethylene glycol)-2000] (ammonium salt) (PEG2000-PE) (CAT# 880150) were from Avanti Polar Lipids. The lipid components were diluted in EtOH before formulation. The nucleic acids, gWiz-GFP plasmid DNA (pDNA), and DasherGFP mRNA were from Aldevron. The nucleic acids were prepared in citrate-buffered saline at pH 4.25. All solvents were LCMS grade and obtained from Burdick and Jackson. Human control plasma was from SCIEX.

LNP Formulation: To produce LNPs, lipids were mixed at a molar ratio of ALC-0315:DSPC:Cholesterol: PEG2000-lipid 46.3:9.4:42.7:1.6. LNPs were formulated with a NanoAssemblr Ignite microfluidic device from Cytiva using a 10 mL/min flow rate and a 3:1 mixing ratio of aqueous citrate buffer, which contains the nucleic acid, to EtOH, which contains the lipid mixture. Following formulation, LNPs were diluted with phosphate-buffered saline and a buffer exchange was performed using 100kDa molecular weight cut-off ultracentrifugal filters.

Sample preparation: ALC-0315 and LNPs were diluted into plasma. Samples were extracted by protein precipitation by adding 100% ACN, followed by benchtop centrifugation for 10 minutes. Supernatants were collected, and 2 mL were injected into the LC column for LC-MS/MS analyses.

Chromatography: Extracts were analyzed on a ZenoTOF 7600 system using an Exion UHPLC. Samples were separated with a Peptide BEH C18 column (150 x 2.1 mm; 1.7 µm, 130 A, Waters, P/N:186003687). Chromatographic gradient details are shown in **Table 1.** The autosampler and column oven temperatures were 15 °C and 70 °C, respectively. The mobile phase flow rate was 0.5 mL/min, and the total run time was 27 min. Mobile phases A and B consisted of 10 mM ammonium acetate in water/MeOH/ACN (15/30/55; v/v) and 10 mM ammonium acetate in ACN/MeOH (60/40; v/v), respectively.

Table 1. Chromatographic gradient (flow rate = 500 µL/min)

Time (min)	Mobile phase A (%)	Mobile Phase B (%)
0	100	0
2	100	0
11	0	100
21	0	100
21.1	100	0
27	100	0

Mass spectrometry: All analyses were performed using the ZenoTOF 7600 system with an OptiFlow Turbo V ion source. Data for the ALC-0315 standard curve and the quantitation of ALC-0315 from formulated LNPs were acquired with TOF-MS and high-resolution MRM (MRM^{HR}) using either precursor-to-precursor (m/z 766.7 to 766.7) or CID-based precursor-to-fragment (m/z 766.7 to 510.5) transitions. (Instrument parameters are shown in **Table 2**.) The external calibration curves were derived from three separate injections for each concentration. The amount of ALC-0315 from LNPs was estimated from these curves. Impurities related to ALC-0315 from LNPs were identified from a data-dependent acquisition (DDA) experiment, termed IDA, after initial dilution into MeOH

(**Table 3**). An MRM^{HR} target list using CID- or EAD-based fragmentation for these impurities was then incorporated into an MRM^{HR} method for impurity analysis of ALC-0315 after diluting the LNPs into plasma (**Table 4**).

Table 2: ZenoTOF 7600 system parameters for quantitation by MRM^{HR}

Parameter	ZenoTOF 7600 system setting
Curtain gas (CUR)	35
Ion source gas 1 (GS1)	60
Ion source gas 2 (GS2)	80
CAD Gas (CAD)	7
Source temperature (TEM)	450 °C
Ion spray voltage (IS)	5500 V
Declustering Potential (DP)	60 V
TOF MS Accumulation time	0.1 s
TOF MS Collision energy (CE)	10 V
TOF MS mass range	100-1200 Da
TOF MS/MS Accumulation time	0.035 s
TOF MS/MS CE	12 V
TOF MS/MS mass range	100-1000 Da
Time bins to sum (TOF MS; TOF MS/MS)	6;6
Zeno pulsing for MS/MS	Yes
Zeno threshold	20000

Table 3: ZenoTOF 7600 system parameter settings for IDA

Parameter	ZenoTOF 7600 system setting
Curtain gas (CUR)	35
Ion source gas 1 (GS1)	60
Ion source gas 2 (GS2)	80
CAD Gas (CAD)	7
Source temperature (TEM)	450 °C
Ion spray voltage (IS)	5500 V
Declustering Potential (DP)	60 V
TOF MS Accumulation time	0.1 s
TOF MS Collision energy (CE)	10 V
TOF MS mass range	100-1200 Da
TOF MS/MS Accumulation time	0.095 s
Electron Beam Current	4000 nA
EAD reaction time	0.03 s
Electron KE	15 eV
TOF MS/MS CE	12 V
TOF MS/MS mass range	20-1200 Da
Time bins to sum (TOF MS; TOF MS/MS)	6;6
Zeno pulsing for MS/MS	Yes
Zeno threshold	20000

Data processing: Quantitation data were processed using the Analytic module within SCIEX OS software. The Explorer module of SCIEX OS performed structural characterization of ALC-0315-related impurities from EAD and CID fragment ion spectra.

Results and discussion

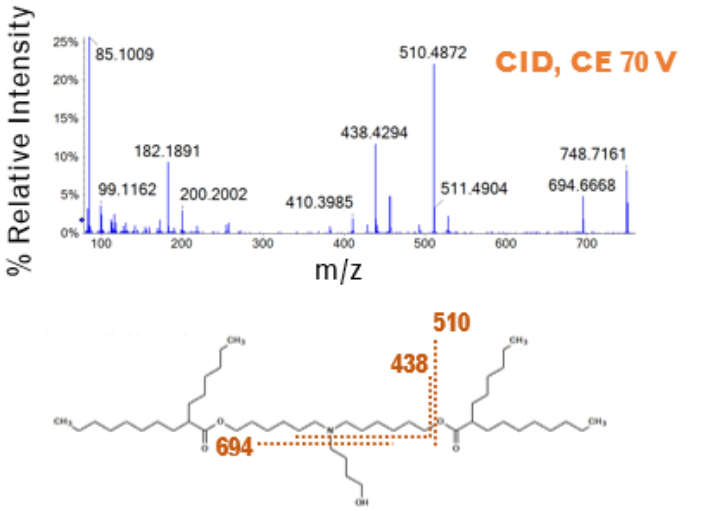

Figure 2. Fragmentation of ALC-0315 by CID. Selected fragment ions at high relative abundance were overlayed on the structure of ALC-0315. Due to the inefficiency of CID-based fragmentation, a precursor-to-precursor MRM transition was used to maximize sensitivity. Note the lack of diagnostic fragments generated using CID, as shown in the chemical structure.

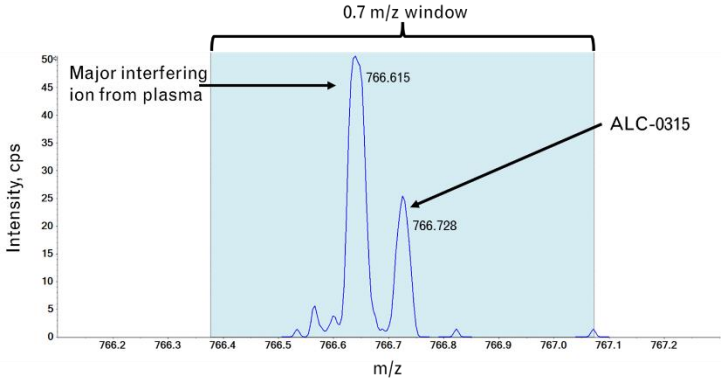

Figure 3. ALC-0315 interferences from plasma matrix. TOF MS analysis of ALC-0315 diluted into plasma shows the presence of ions with similar molecular weights to ALC-0315. The highlight blue box shows a surrounding 0.7 m/z window to represent a typical quadrupole mass analyzer isolation window containing these major interfering ions. This demonstrates the ability of the TOF mass analyzer to provide added selectivity.

Quantitation in biological matrices by LC-MS/MS traditionally relies upon the specificity of precursor-to-fragment MRM experiments using a TQMS. ALC-0315 does not fragment efficiently by CID even after optimizing instrument parameters (**Figure 2**); consequently, it was investigated whether the specificity from HRMS could improve quantitative analysis. For example, the TOF MS spectrum of ALC-0315 diluted into plasma showed an interference from a prominent ion in the matrix observed at m/z 766.650, which is close to the precursor ion of ALC-0315 observed at m/z 766.728 (**Figure 3**). The high-resolution mass analyzer on the ZenoTOF 7600 system can

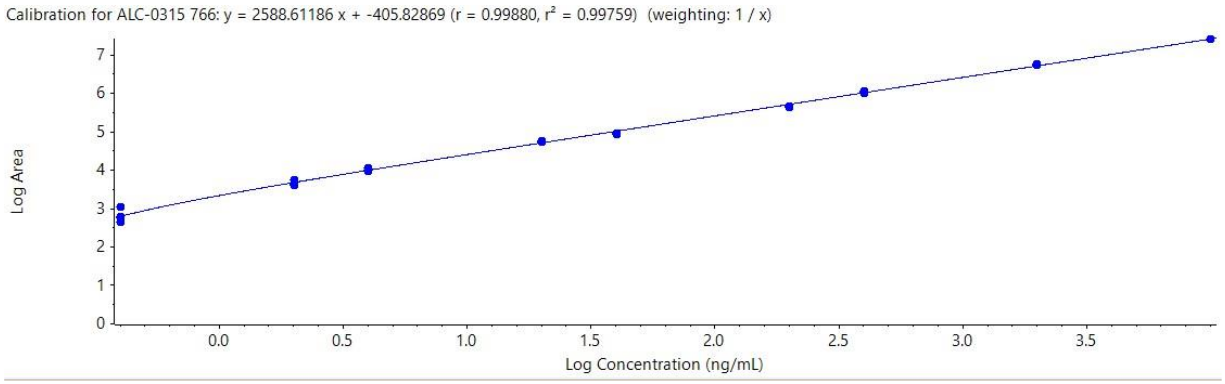

Row	Component Name	Actual Concentration	Num. Values	Mean	Standard Deviation	Percent CV	Average Accuracy across Replicates
1	ALC-0315 766	0.4000	3 of 3	4.304e-1	1.260e-1	29.27	107.60
2	ALC-0315 766	2.0000	3 of 3	1.951e0	2.824e-1	14.47	97.57
3	ALC-0315 766	4.0000	3 of 3	4.067e0	3.356e-1	8.25	101.67
4	ALC-0315 766	20.0000	3 of 3	2.207e1	7.693e-1	3.49	110.33
5	ALC-0315 766	40.0000	3 of 3	3.463e1	8.889e-1	2.57	86.58
6	ALC-0315 766	200.0000	3 of 3	1.693e2	7.166e0	4.23	84.66
7	ALC-0315 766	400.0000	3 of 3	4.141e2	1.976e1	4.77	103.54
8	ALC-0315 766	2000.0000	3 of 3	2.196e3	3.789e1	1.73	109.81
9	ALC-0315 766	10000.0000	3 of 3	9.823e3	9.346e1	0.95	98.23

Figure 4. Quantitative calibration curve of ALC-0315 in plasma using precursor-to-precursor MRM^{HR} transitions. A quantitation curve (top) was created from various dilutions of ALC-0315 in plasma across over 4 orders of linear dynamic range. The table (bottom) displays quantitative statistics demonstrating the quantitative performance of the ZenoTOF 7600 system

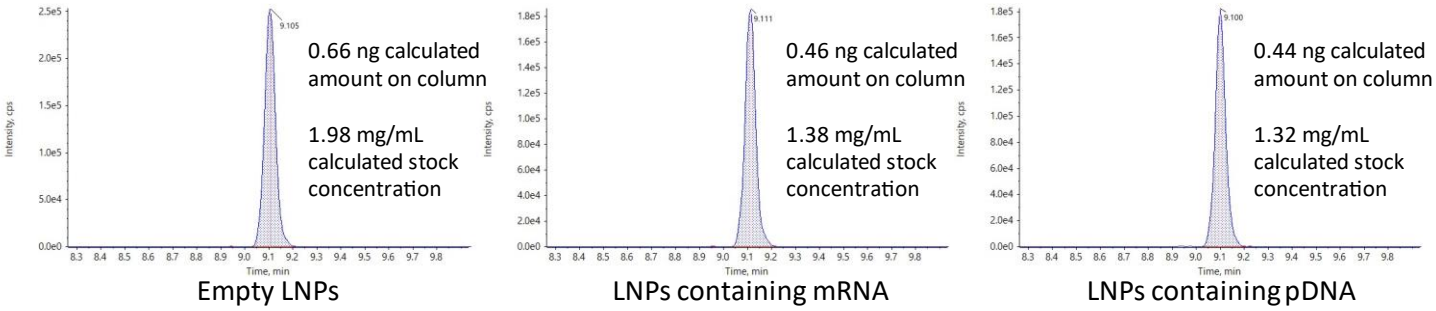

Figure 5. Quantitation of ALC-0315 from LNPs diluted into plasma. Three different preparations of LNPs formulated with or without genetic material were diluted 1:6000 into plasma. The amounts of ALC-0315 from the LNPs were determined using the calibration curve equations from Figure 4.

distinguish this signal, which otherwise would interfere with a TQMS system. The ZenoTOF 7600 system offers high sensitivity MS/MS via the Zeno trap, low detector noise compared to other HRMS systems, and the ability to analyze ions within a narrow extraction window, and we explored whether these attributes could provide specific benefits from different acquisition modes. These included TOF MS to monitor the ALC-0315 precursor, MRM^{HR} of precursor-to-precursor ions, and MRM^{HR} monitoring the 510.486 m/z fragment ion. **Figure 4** shows a dilution curve spanning 4 orders of linearity with high accuracies from the precursor-to-precursor MRM^{HR} experiment. This experiment yielded greater sensitivity with a 0.4 ng/mL LLOQ, which was 5x lower than precursor-to-fragment MRM^{HR} (**Figure 1**).

After establishing the quantitative methodology for ALC-0315, we applied this to formulated LNPs. LNPs were diluted in methanol and subjected to LC-MS analysis for initial assessment. All components of the LNPs were observed, including ALC-0315 and the PEGylated lipid (**Figure 6**). This indicated that a bioanalytical method could be developed for other exogenous materials like the PEGylated lipid in addition to the ionizable lipid using this methodology.

The amounts of ALC-0315 from three different preparations of LNPs diluted into plasma were measured to assess the quantitative performance of the ZenoTOF 7600 system. The LNPs were initially formulated with mRNA, pDNA, or they were empty. The peak areas of the ALC-0315 detected from these LNP preparations diluted 1:6000 are shown in **Figure 5**. The concentrations of ALC-0315 from 3 LNP preparations were calculated as 0.33, 0.23, and 0.22 mg/mL, based on the external calibration curve from **Figure 4**. These measurements estimated the original stock concentrations to range from 1.32 to 1.98 mg/mL by extrapolation. This is consistent

with the amount of ALC-0315 initially used in the LNP formulation, allowing for some moderate sample loss, where 20-50% lipid loss from filtration (e.g., dialysis) is typical (14-15). A dilution of 1:6000 was 1000x higher than the LLOQ, demonstrating the sensitivity of the ZenoTOF 7600 system. Overall, this method is suitable for measuring trace amounts of material for thorough and sensitive biodistribution assessments.

During the initial analysis of the LNPs, we also observed several low-level impurities (**Figure 6, inset with zoomed x and y axes**). These analytes were noted and analyzed to assess the utility of the ZenoTOF 7600 system in supporting MetID studies using EAD. Previously, using positive ion mode LC-MS/MS, ALC-0315 was shown to undergo biotransformation via hydrolysis to m/z 528.4986 (16). We also observed a peak at m/z 528.4999 from the impurity profile. From the other impurities found, chemical formulae were deduced based on precursor masses listed in **Table 4**.

The ZenoTOF 7600 system can perform low-energy electron impact fragmentation (electron impact excitation of ions from organics; EIEIO) using the EAD cell. EIEIO is especially useful for elucidating lipid structures because it generates significantly more fragment

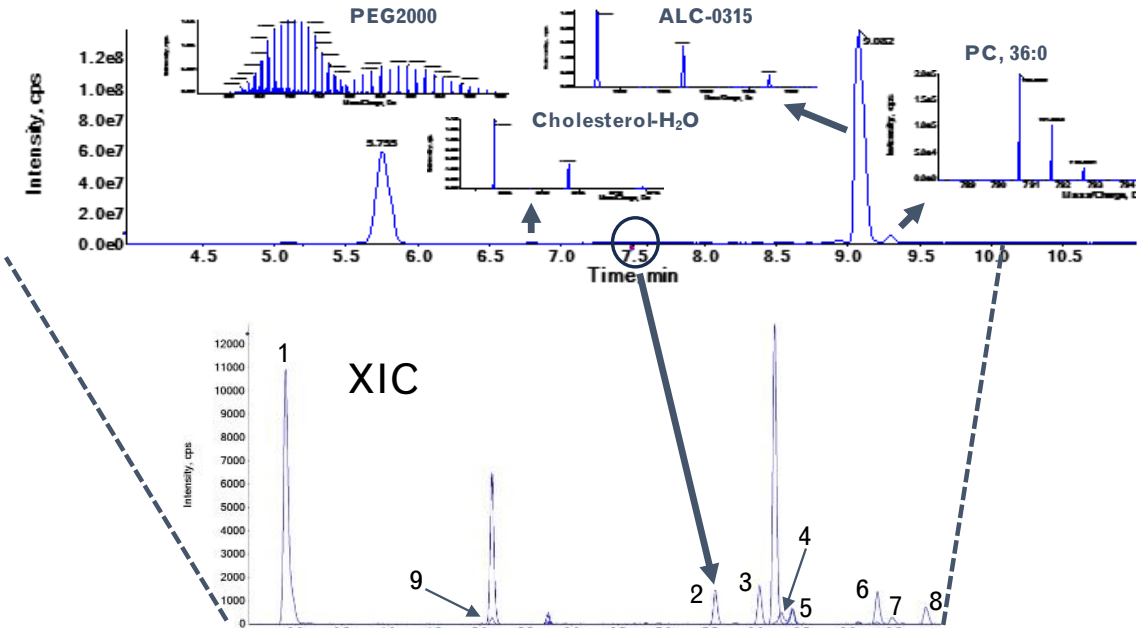

Figure 6. TOF MS analysis of LNPs. TOF MS of LNPs using the ZenoTOF 7600 system was able to detect all the lipid components of the LNPs, including several low-level impurities related to ALC-0315

Table 4. Precursor ions and their masses from impurity profile experiment (Figure 6)

Compound ID	Precursor ion
ALC-0315 60	*766.728*
N-Oxide	*782.723*
Head	*694.671*
Side	*428.410*
One ester	*556.494*
Unknown 611	*611.547*
Unknown 814	*814.705*
Unknown 748	*748.717*
Unknown 738	*738.696*
Unknown 762	*762.601*
Unknown 752	*752.712*
Unknown 764	*764.712*
Unknown 722	*722.702*
Unknown 780	*780.743*
Unknown 794	*794.759*
Unknown 822	*822.791*
Unknown 1032	*1032.989*
Unknown 1105	*1105.047*

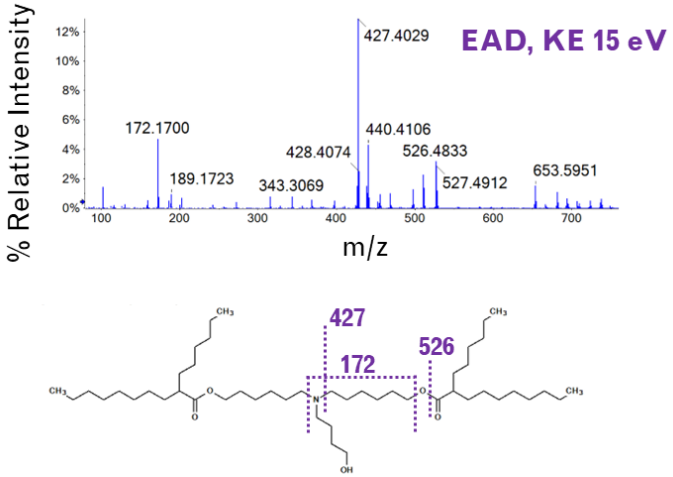

Figure 7. Fragmentation of ALC-315 by EAD. Compared to the CID spectrum, EAD produces product ion spectra that denote more structural detail and can be used to better characterize this type of compound.

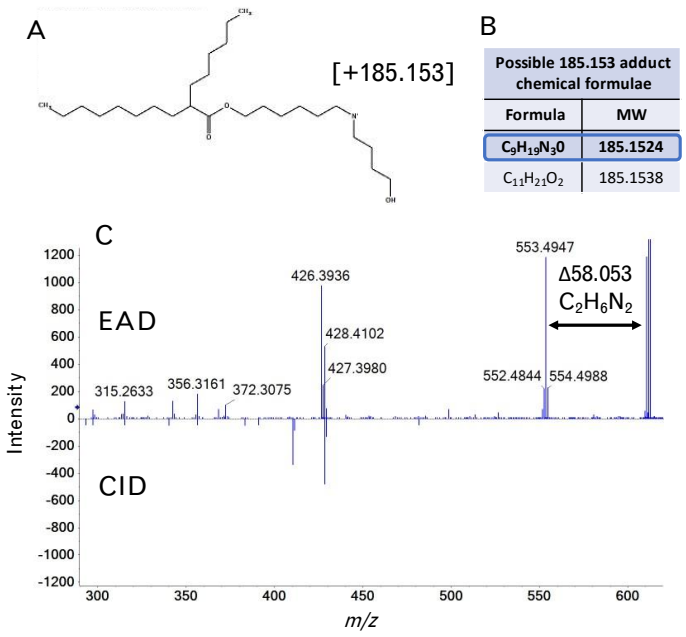

Figure 8. Deduction of unknown chemical adduct to an ALC-0315 impurity from plasma using EAD. A unique impurity with a precursor m/z 610.54 was observed. Initial interpretation from a fragment ion spectrum revealed a loss of one of the hexane-6,1-diyl) bis(2-hexyldecanoate) chains of ALC-0315 and the addition of an unknown adduct of 185.153 MW (A), which could be represented by two different chemical formulae based on accurate mass (B). (C) Fragmentation by EAD uniquely produced a m/z 553.495 fragment ion that could only result from loss of a nitrogen containing moiety - $C_6H_6N_2$. By process of elimination, the unknown adduct formula was determined to be $C_9H_{19}N_3O$.

ions than other fragmentation techniques like CID (**Figures 2 and 7**) (8,9,11, 12). This technique was previously used to elucidate structures related to ALC-0315 (12) confidently.

EIEIO-based fragmentation was used on selected impurities of ALC-0315 after LNP dilution into plasma. Unique fragments of m/z 187.156, 443.397, and 709.656 were observed for an oxidative impurity of m/z 781.716 by EIEIO, which were not seen by CID. (**Figure 1, lower right**). These fragments were used to pinpoint oxygen incorporation to a specific, confined region surrounding the tertiary amine within the structure of ALC-0315, strongly suggesting that this impurity was the N-oxide of ALC-0315.

A more complex unknown impurity at m/z 610.540 was also observed. This molecular weight is consistent with the loss of one of the hexane-6,1-diyl bis(2-hexyldecanoate) ($C_{22}H_{44}O_2$) chains, and the addition of an unknown covalent addition with a molecular weight of 185.153 (**Figure 8A**). This molecular weight could be explained by two different chemical formulae based solely on MS accurate mass – $C_9H_{19}N_3O$ or $C_{11}H_{21}O_2$, as shown in **Figure 8B**. Fragmentation by EAD resulted in a unique fragment of m/z 553.494 not seen by CID, which was 58.053 mass units less than the precursor molecular weight (**Figure 8C**). This loss could only be explained by a nitrogen-containing chemical formula of $C_2H_6N_2$ due to accurate mass measurement and the mass defect of molecular nitrogen. In addition, fragment ions matching losses relating to the chemical formulae of $C_8H_{19}N_2$ and $C_9H_{21}N_2$ were also observed in the EAD fragment ion spectrum. As a result, the adducted chemical formula was narrowed down to $C_9H_{19}N_3O$. Although it is difficult to derive the exact structure of this adduct, these data show that EAD provides valuable information that is not attainable by accurate mass measurements or by CID alone. This information could help corroborate the elucidation of other unknown lipid-adducted species from oligonucleotide or protein modifications.

The ZenoTOF 7600 system provides tremendous versatility to support in-depth and sensitive LC-MS/MS-based DMPK studies. The resolution, sensitivity, and dynamic range enabled a quantitation curve of ALC-0315 in plasma of over 4 orders of linearity with an LLOQ of 0.4 ng/mL using a precursor-to-precursor MRM transition. This experiment overcame the CID-based fragmentation inefficiency of ALC-0315 that would be encountered on a TQMS system while still providing the necessary specificity to support bioanalysis from the plasma matrix. In addition, EAD fragmentation provides definitive structural information on lipid impurities from LNPs. This information could help identify process-related impurities formed *during LNP manufacturing and formulation or biotransformations to* support MetID studies.

Conclusions

- The sensitivity of the ZenoTOF 7600 system enables the low-level detection and quantitation of lipids related to LNPs in plasma to support quantitative bioanalysis in complex matrix
- Fragmentation of ionizable lipids and their related impurities using EAD results in information-rich product ion spectra even at low abundance after dilution into plasma
- Unique fragment ions of impurities related to ALC-0315 from EAD can be used to confidently identify these analytes and pinpoint sites of modification, demonstrating that this technique can support and benefit metabolism studies
- Sensitive quantitation paired with detailed structural characterization shows the versatility of the ZenoTOF 7600 system to support multiple workflows within DMPK

References

1. Che P, Davidson JT, Kool J, Kohler I. *Electron activated dissociation – a complimentary fragmentation technique to collision-induced dissociation for metabolite identification of synthetic cathinone positional isomers.* Anal Chim Acta. 2023; Dec 1;1283 1-12. doi: 10.1016/j.aca.2023.341962
2. Calabrese V, Brunet TA, Degli-Esposti D, Chaumot A, Geffard O, Salvador A, Clement Y, Ayciriex S. *Electron-activated dissociation (EAD) for the complementary annotation of metabolites and lipids through data-dependent acquisition analysis and feature-based molecular networking, applied to the sentinel amphipod Gammarus fossarum.* Anal Bioanal Chem. 2024; May;416(12):2893-2911. doi 10.1007/s00216-024-05232-w
3. He Y, Hou P, Long Z, Zheng Y, Tang C, Jones E, Diao X, Zhu M. *Application of electro-activated dissociation fragmentation technique to identifying glucuronidation and oxidative metabolism sites of vepdegestrant by liquid chromatography-high resolution mass spectrometry.* Drug Metab Dispos. 2024; Jun 17;52(7):634-643. doi 10.1124/dmd.124.001661
4. Baba T, Campbell JL, Le Blanc JCY, Baker PRS. *In-depth sphingomyelin characterization using electron impact excitation of ions from organics and mass spectrometry.* J Lipid Res. 2016; May;57(5):858-67. doi 10.1194/jlr.M067199
5. Baba T, Campbell JL, Le Blanc JCY, Baker PRS. *Distinguishing cis and trans isomers in intact complex lipids using electron impact excitation of ions from organics mass spectrometry.* Anal Chem. 2017; Jul 18;89(14):7307-7315. doi: 10.1021/acs.analchem.6b04734
6. Baba T, Campbell JL, Le Blanc JCY, Baker PRS. *Structural identification of eicosanoids with ring structures using differential mobility spectrometry-electron impact excitation of ions from organics mass spectrometry.* J Am Soc Mass Spectrom. 2023; Jan 4:34(1);75-81. doi: 10.1021/jasms.2c00256
7. Baba T, Campbell JL, Le Blanc JCY, Baker PRS. *Structural identification of triacylglycerol isomers using electron impact excitation of ions from organics (EIEIO).* J Lipid Res. 2016; Nov;57(11);2015-2027. doi: 10.1194/jlr.M070177
8. Pearson M, Hunter C, Baba T. Complete structural elucidation of lipids in a single experiment using electron activated dissociation (EAD). SCIEX technical note, RUO-MKT-02-13050-B
9. Jinmei C, Dandan S, Zhimin L, Lihai G. Systematic determination of lipid structure using electron activated dissociation (EAD). SCIEX technical note, RUO-MKT-02-14182-A
10. Chaudhary N, Weissman D, Whitehead KA. *mRNA vaccines for infectious diseases: principles, delivery and clinical translation.* Nat Rev Drug Discov 2021; Nov;20(11):817–838. doi: 10.1038/s41573-021-00283-5
11. Crowe A, Jain N, Higgins R, Proos R, Stone M, Pohl K. Distinguishing oxidative impurities from ionizable lipids used in LNP formulations using electron activated dissociation. SCIEX technical note, RUO-MKT-02-14983-A
12. Yang Z, Baker P, Mollah S, Proos R, Le Huray J. Structural characterization of the cationic lipid nanoparticle component, ALC-0315, and its impurities using electron-activated dissociation (EAD)-based MS/MS fragmentation. SCIEX technical note, RUO-MKT-26966-A
13. Yang Z, Mollah S, Kaluarachchi H, Jin W, Al-Dulaymi M. Automated characterization of the lipid nanoparticle ionizable lipid, DODAP, and its degradants using Molecule Profiler software. SCIEX technical note, RUO-MKT-26226-A
14. De Peña AC, Zimmer D, Gutterman-Johns E, Chen NM, Tripathi A, Bailey-Hytholt CM. *Electrophoretic microfluidic characterization of mRNA- and pDNA-loaded lipid nanoparticles.* ACS Appl Mater Interfaces. 2024; May 29;16(21):26984-26997. doi: 10.1021/acsami.4c00208
15. Mousli Y, Brachet M, Chain JL, Ferey L. *A rapid and quantitative reversed-phase HPLC-DAD/ELSD method for lipids involved in nanoparticle formulations.* J Pharm Biomed Anal. 2022; Oct 25:220:115011. doi: 10.1016/j.pba.2022.115011
16. https://downloads.regulations.gov/CDC-2021-0034-1148/attachment_1.pdf

The SCIEX clinical diagnostic portfolio is For In Vitro Diagnostic Use. Rx Only. Product(s) not available in all countries. For information on availability, please contact your local sales representative or refer to **https://sciex.com/diagnostics.** All other products are For Research Use Only. Not for use in Diagnostic Procedures.

Headquarters
500 Old Connecticut Path | Framingham, MA 01701
USA
Phone 508-383-7700
sciex.com

International Sales
For our office locations please call the division headquarters or refer to our website at
sciex.com/offices